Inorganic Chemistry

pubs.acs.org/IC

Forum Article

Progressing the Frustrated Lewis Pair Abilities of N-Heterocyclic Carbene/GaR_3 Combinations for Catalytic Hydroboration of Aldehydes and Ketones

Leonie J. Bole, Marina Uzelac, Alberto Hernán-Gómez, Alan R. Kennedy, Charles T. O'Hara, and Eva Hevia*

Cite This: https://doi.org/10.1021/acs.inorgchem.1c01276

Read Online

ACCESS | Metrics & More | Article Recommendations | Supporting Information

ABSTRACT: Exploiting the steric incompatibility of the tris(alkyl)gallium GaR_3 (R = CH_2SiMe_3) and the bulky N-heterocyclic carbene (NHC) 1,3-bis(*tert*-butyl)imidazol-2-ylidene (I*t*Bu), here we report the B−H bond activation of pinacolborane (HBPin), which has led to the isolation and structural authentication of a novel ion pair, $[\{I^tBu\text{-}BPin\}^+\{GaR_3(\mu\text{-}H)GaR_3\}^-]$ (**2**). Contrastingly, neither I*t*Bu or GaR_3 was able to react with HBPin under the conditions of this study. Combining an NHC-stabilized borenium cation, $[\{I^tBu\text{-}BPin\}^+]$, with an anionic dinuclear gallate, $[\{GaR_3(\mu\text{-}H)GaR_3\}^-]$, **2** proved to be unstable in solution at room temperature, evolving to the abnormal NHC-Ga complex $[BPinC\{\{N(tBu)\}_2CHGa(R)_3\}]$ (**3**). Interestingly, the structural isomer of **2**, with the borenium cation residing at the C4 position of the carbene, $[\{aI^tBu\text{-}BPin\}^+\{GaR_3(\mu\text{-}H)GaR_3\}^-]$ (**4**), was obtained when the abnormal NHC complex $[aI^tBu{\cdot}GaR_3]$ (**1**) was heated to 70 °C with HBPin, demonstrating that, under these forced conditions, it is possible to induce thermal frustration of the Lewis base/Lewis acid components of **1**, enabling the activation of HBPin. Building on these stoichiometric studies, the frustrated Lewis pair (FLP) reactivity observed for the GaR_3/I*t*Bu combination with HBPin could then be upgraded to catalytic regimes, allowing the efficient hydroboration of a range of aldehydes and ketones under mild reaction conditions. Mechanistic insights into the possible reaction pathway involved in this process have been gained by combining kinetic investigations with a comparative study of the catalytic capabilities of several gallium and borenium species related to **2**. Disclosing a new cooperative partnership, reactions are proposed to occur via the formation of a highly reactive monomeric hydride gallate, $[\{I^tBu\text{-}BPin\}^+\{GaR_3(H)\}^-]$ (**I**). Each anionic and cationic component of **I** plays a key role for success of the hydroboration, with the nucleophilic monomeric gallate anion favoring the transfer of its hydride to the C═O bond of the organic substate, which in turn is activated by coordination to the borenium cation.

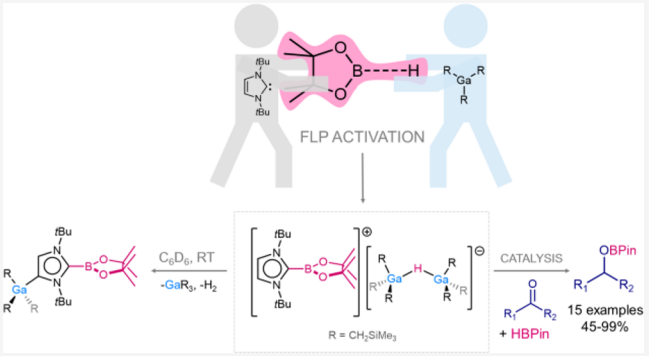

INTRODUCTION

Since the inception of frustrated Lewis pair (FLP) chemistry,[1] sterically incompatible Lewis acid/base (LA/LB) pairings have become a powerful and widespread protocol for the activation of small molecules,[2] which in some cases can be upgraded from stoichiometric conditions to catalytic regimes.[3] Some of the most popular FLP systems have been modeled from the classical phosphine/borane combinations, where the borane often contains strongly electron-withdrawing and sterically encumbering perfluoroarene (Ar^F) substitutents.[4] However, deviations from the phosphine/borane systems that explore, for instance, N-heterocyclic carbenes (NHCs) as the Lewis basic component[5] or aluminum complexes[6] as an alternative Lewis acid choice are possible. Despite the significant use of Lewis acidic group 13 elements B and Al, Ga has been significantly less employed.[7] Recently, we have shown that, by combining the particularly bulky and basic NHC 1,3-di-*tert*-butylimidazol-2-ylidene (I*t*Bu) with tris(alkyl)gallium GaR_3 (R = CH_2SiMe_3), it is possible to activate unsaturated organic molecules such as ketones and aldehydes (via C═O insertion)[8] as well as the cleavage of X−H acidic bonds of alcohols, amines, and acetylenes, to name just a few.[9] When structural studies were combined with NMR spectroscopic monitoring of the reactions and density functional theory (DFT) calculations, our previous studies shed new light on the possible mechanisms involved in C═O reduction processes,

Special Issue: Advances in Small-Molecule Activation

Received: April 26, 2021

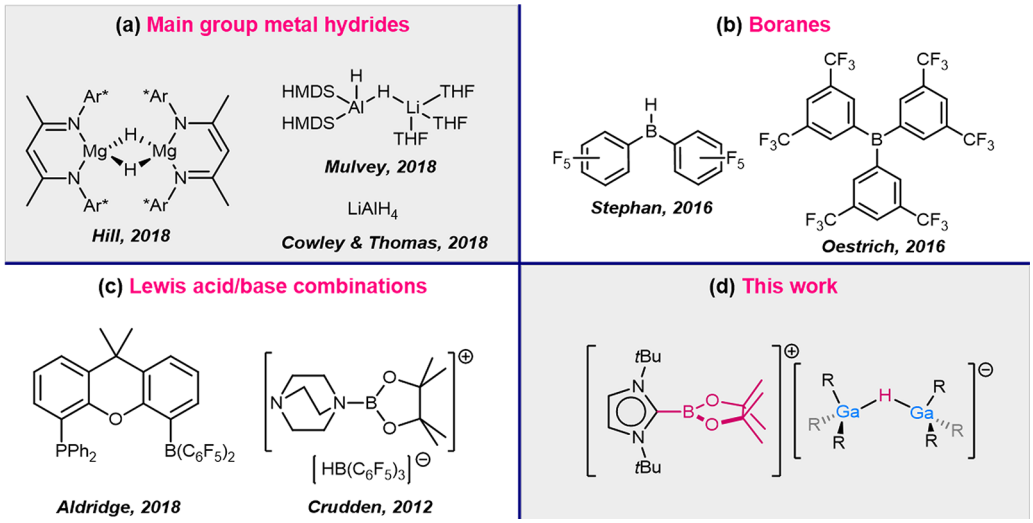

Figure 1. Selected examples of main-group catalytic approaches for hydroboration reactions. Ar* = 2,6-$(iPr)_2$-C_6H_3, HMDS = $N(SiMe_3)_2$, and R = CH_2SiMe_3.

Scheme 1. (a) Synthesis of 1 and (b) Synthesis of 2 via FLP Splitting of HBPin

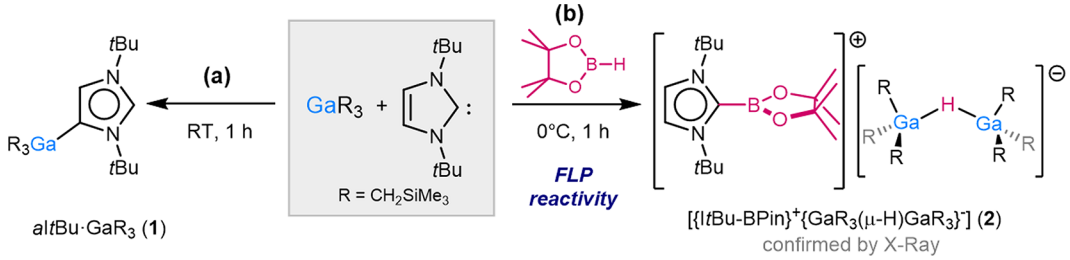

where the NHC can act as a Lewis base not only via its *normal* C2 position (kinetic product) but also via its C4 (*abnormal*) site (thermodynamic product). This isomerization seems to be driven by the relief of the steric hindrance around the new C−O group.[10] Evidencing the synergistic behavior of these NHC/GaR_3 pairings, when separated, none of the components are able to activate these ketones or aldehydes on their own. Building on these studies, here we assess the capabilities of the I*t*Bu/GaR_3 combination to induce the activation of hydridic B−H bonds using HBPin as a model substrate. Furthermore, we also investigate its ability to operate under catalytic conditions to facilitate hydroboration of carbonyl compounds.

Involving the direct addition of a B−H bond across unsaturated organic compounds (i.e., alkenes, alkynes, or carbonyl derivatives), hydroboration catalysis has gained increasing importance in synthesis, becoming a fundamental tool to access organoborane compounds.[11] While a large number of these studies used transition-metal complexes as catalysts, the past decade has witnessed several examples of s- and p-block metal hydrides (Figure 1a) that have emerged as competent hydroboration catalysts toward a variety of unsaturated substrates, with the vast majority of these studies using HBPin as the borane of choice.[12−17] For carbonyl-based substrates, these reactions are generally accepted to proceed through an initial insertion of the substrate across the metal−hydride bond, leading to an alkoxide intermediate. A σ-bond metathesis step can then ensue, promoted by the stoichiometric excess of HBPin present, leading to the final product with regeneration of the active hydride catalyst. Metal-free examples have also been established in recent years, with examples from Stephan et al.[18] and Oestreich et al.[19] that have shown that electrophilic boranes such as Piers' borane $[HB(C_6F_5)_2]$ and $B(3,5\text{-}(CF_3)_2\text{-}C_6H_3)_3$ are able to catalyze the hydroboration of alkenes and alkynes with HBPin (Figure 1b). This approach has also been used for hydroboration of imines, ketones, aldehydes, and alkynes, where a series of system-specific mechanisms have been proposed to be in operation.[20] Not limited to single-component systems, highly Lewis acidic boranes, such as the tris(pentafluorophenyl)-borane $B(C_6F_5)_3$, in the presence of a Lewis base (Figure 1c) can perform activation of the B−H bond of HBPin, leading to ion-pair intermediates,[21,22] often described as $[HB(C_6F_5)_3]^-$ balanced by the borenium cation $[LB{\cdot}BPin]^+$. The latter has been proposed to actually be the active catalyst in studies by Crudden et al. when using 1,4-diazabicyclo[2.2.2]octane (DABCO) as a LB for the hydroboration of imines (Figure 1c).[21]

Herein we investigate the catalytic ability of a novel gallium hydride species (Figure 1d) obtained by the activation of HBPin using I*t*Bu/GaR_3 (vide infra) to facilitate the hydroboration of ketones, aldehydes, and imines. Through the isolation of key reaction intermediates and kinetic studies, we have provided mechanistic insights into how these processes may take place.

RESULTS AND DISCUSSION

Taking heed from our previous studies,[23] combining equimolar amounts of GaR_3 and I*t*Bu in a nonpolar solvent at room temperature instantly leads to the formation of a stable, abnormal NHC/Ga complex, *a*I*t*Bu·GaR_3 (**1**; Scheme 1a). The

https://doi.org/10.1021/acs.inorgchem.1c01276
Inorg. Chem. XXXX, XXX, XXX−XXX

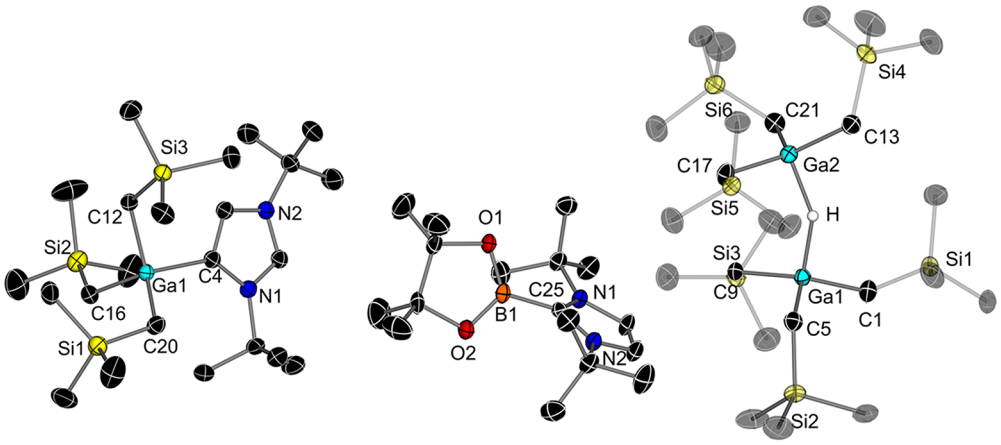

Figure 2. Molecular structures of **1** and **2** with displacement ellipsoids at 50% probability and all H atoms omitted for clarity, with the exception of the bridging hydride of **2**. $SiMe_3$ groups have been drawn at 70% transparency for clarity. Selected bond angles (deg) and distances (Å) of **1**: C12−Ga1−C16 108.96(7), C12−Ga1−C20 112.18(8), C12−Ga1−C4 103.09(7), C16−Ga1−C2 110.70(7), C16−Ga1−C4 108.29(7), C20−Ga1−C4 113.27(7); Ga1−C12 2.0255(17), Ga1−C16 2.0231(18), Ga1−C20 2.0154(18), Ga1−C4 2.0771(17). Selected bond angles (deg) and distances (Å) of **2**: O1−B1−C25 120.46(19), O2−B1−C25 123.79(19), O2−B1−O2 115.73(19), N1−C25−B1 126.47(18), N1−C25−N2 107.35(17), B1−C25−N2 125.92(19); Ga1−C1 2.004(2), Ga1−C5 2.010(2), Ga1−C9 2.012(2), B1−C25 1.588(3).

structure of **1** was established by X-ray crystallographic studies (Figure 2), and it can be considered to be a deactivation product because, at room temperature, it is a highly robust species that shows no dissociation or further FLP reactivity. However, in our previous work, we discovered that its formation can be minimized by lowering the reaction temperature to 0 °C. Introducing a suitable substrate under these conditions could then promote its subsequent activation (via X−H activation or C═O insertion).[8,9] Thus, we started our stoichiometric studies by reacting HBPin with equimolar amounts of GaR_3 and I*t*Bu at 0 °C for 1 h in hexane. Cooling the solution to −30 °C led to isolation of the borenium gallate complex $[\{I\textit{t}Bu\text{-}BPin\}^+\{GaR_3(\mu\text{-}H)GaR_3\}^-]$ (**2**), which was characterized by X-ray crystallographic analysis and can be envisaged to form as a result of the FLP splitting of the B−H bond of borane. The formation of **2** is clearly synergic because no apparent reaction of the individual components is observed with HBPin under those conditions. For I*t*Bu, on its own, not even coordination to HBPin is observed, whereas GaR_3 slowly generates RBPin over long periods of time at room temperature (64% conversion after 2 days).

Compound **2** consists of a cationic NHC-BPin fragment, with the B residing on the C2 position of the carbene (C25 in Figure 2). Both C and B atoms exhibit trigonal-planar environments (the sum of angles around C25 and B1 and 359.75° and 359.98°, respectively). The length of the B1−C25 bond [1.588(3) Å] is consistent with those reported in the literature for related NHC-stabilized bis(aryl)borenium cations.[24] Unsurprisingly, this B−C bond distance is noticeably shorter than that recently reported by Mandal et al. for a coordination adduct between a tetrasubstituted abnormal NHC and HBPin [1.668(2) Å], which can be rationalized considering the higher coordination number of B in the latter and its neutral character in comparison with the borenium cation.[25] Considering the near-perpendicular binding of BPin to the NHC, similarities can be drawn to an example reported by Vidović et al., where I*t*Bu is used to stabilize a catecholatoborenium cation, [{BCat$^+$}], with charge balance achieved by a $[\{B(3,5\text{-}Cl_2\text{-}C_6H_3)_4\}^-]$ anion.[26] The authors comment that the side-on arrangement of the borenium to the NHC allows for electrostatic interactions between Me groups of the NHC's *t*Bu substituents and the cationic B atom, with a mean distance of 2.846 Å. Within **2**, it is therefore likely that the orthogonal binding of [{BPin}$^+$] to the NHC maximizes the opportunity for stabilization of the borocation via interaction of the Me groups to the empty p orbital of B with detected distances of 3.081(4) and 3.028(3) Å from the crystallographic data.

While discussions thus far have labeled $[\{I\textit{t}Bu\text{-}BPin\}^+]$ as a borenium cation, it could also be formally considered to be a borylimidazolium cation (Scheme 2). Previous theoretical

Scheme 2. Borenium and Imidazolium Representations of $[\{I\textit{t}Bu\text{-}BPin\}^+]$ of 2

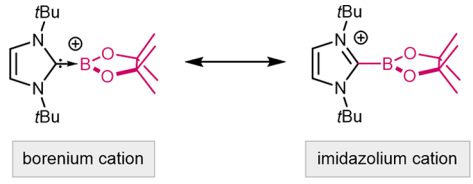

studies by Stephan et al. have focused on a constitutionally analogous species to **2**, reached by FLP activation of catecholborane by $t\text{Bu}_3\text{P}$ and $B(C_6F_5)_3$, leading to the ion pair $[\{t\text{Bu}_3\text{P-BCat}\}^+\{HB(C_6F_5)_3\}^-]$.[4a] Natural bond order calculations then predicted that the charge of the cation formally lies on the P atom, rendering the species as a borylphosphonium rather than a phosphine-stabilized borenium cation. Although a similar understanding could be applied to the cation of **2**, onward reactivity of our system suggests that under catalytic conditions the $[\{I\textit{t}Bu\text{-}BPin\}^+]$ fragment can react as a borenium cation (vide infra).

The counterion for this structure is a dinuclear gallate comprising two GaR_3 units connected by a bridging hydride. The structure of this anion is closely related to that reported by

https://doi.org/10.1021/acs.inorgchem.1c01276
Inorg. Chem. XXXX, XXX, XXX−XXX

Scheme 3. (a) Decomposition Pathway of 2 into 3 by Deprotonation of the Imidazole Backbone and (b) Decomposition of 4 into 5 by Nucleophilic Addition across the C2 Position of the Imidazole Fragment

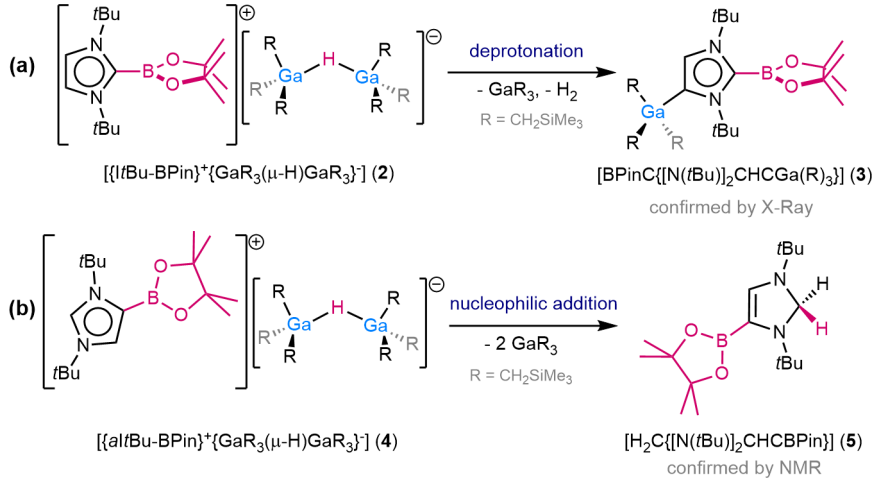

Stephan et al. for $[\{Ga(C_6F_5)_3(\mu\text{-}H)Ga(C_6F_5)_3\}^-]$, which is part of a phosphonium gallate resulting from the FLP cleavage of H_2 by a 2:1 combination of $Ga(C_6F_5)_3$ and P*t*Bu$_3$.[27] Interestingly, despite employment of a 1:1:1 stoichiometry, the anionic fragment of **2** consistently forms with 2 equiv of GaR_3, which we propose to be a crystallization feature for improved stability of the metal hydride species.[28]

While the synthesis and solid-state determination of **2** by X-ray crystallography is reproducible, its isolation at room temperature as a crystalline solid and subsequent solution-state characterization proved particularly challenging, with multiple attempts resulting in decomposition products. Deeper analysis of the products of decomposition revealed the formation of an unexpected abnormal NHC-Ga complex, [BPinC{{N-(*t*Bu)]$_2$CHCGa(R)$_3$}] (**3**), which can be recrystallized in 17% yield (Scheme 3). Its most salient NMR spectroscopic feature is a singlet at 7.32 ppm in the ^{1}H NMR spectrum in C_6D_6 for the remaining H on the imidazole ring, alongside the inequivalence of the *t*Bu groups (at 1.64 and 1.26 ppm). In addition, a resonance at 160.3 ppm is observed in the ^{13}C NMR spectrum for its carbenic C, a chemical shift similar to that observed for **1** (159.5 ppm), whereas its ^{11}B NMR shows a broad resonance at 26.8 ppm, which compares well with neutral BPin-Csp^2 environments.[20b] The structure of **3** could also be established by X-ray crystallographic studies (Figure 3). The key coordination parameters around Ga are similar to those found in **1**, with similar $C_{carbenic}$−Ga distances [2.0771(17) and 2.0852(15) Å, respectively], whereas the B−C2 distance [1.591(2) Å] is almost identical with that found in **2**. While the decomposition of **2** into **3** could not be monitored by NMR spectroscopy, during analysis of isolated samples of **3** by ^{1}H NMR spectroscopy, variable amounts of GaR_3 could also be detected (see the Supporting Information, SI). A possible explanation for the formation of **3** could be deprotonation of the imidazole backbone of **2** by the $[\{GaR_3(\mu\text{-}H)\text{-}GaR_3\}^-]$ fragment, producing a carbenic center at the C4 position to which GaR_3 can then bind with subsequent H_2 elimination (Scheme 3a). This is somewhat surprising because gallium hydrides are expected to be poor bases, but perhaps its anionic constitution enhances its basicity. No evidence could be found to support deprotonation of the imidazole backbone by one of the alkyl groups on Ga, which is consistent with their previously noted low kinetic basicity when coordinated to Ga.[9,29]

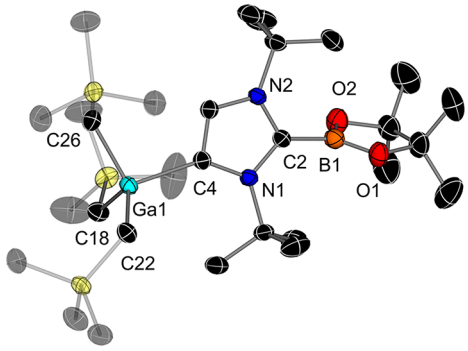

Figure 3. Molecular structure of **3** with displacement ellipsoids at 50% probability and H atoms omitted for clarity. $SiMe_3$ groups have been drawn at 70% transparency for clarity. Selected bond angles (deg) and distances (Å): N2−C2−N1 106.79(12), N2−C2−B1 123.65(12), N1−C2−B1 128.54(13), O2−B1−C2 119.73(15), O2−B1−O1 115.27(15), C2−B1−O1 125.00(15); C2−B1 1.591(2), Ga1−C4 2.0852(2).

As mentioned above, our previous studies have found that **1** is deactivated toward exhibiting further FLP reactivity. A similar behavior has been reported by Tamm et al. for the related *aIt*Bu·B$(C_6F_5)_3$.[30] Interestingly, while **1** is inert towards HBPin at room temperature, we found that increasing the reaction temperature to 70 °C for 4 h allowed for formation of the mixed borenium gallate $[\{aItBu\text{-}BPin\}^+\{GaR_3(\mu\text{-}H)\text{-}GaR_3\}^-]$ (**4**; Figure 4). Compound **4** was subjected to Hirshfeld atom refinement (HAR),[32,33] using the NoSpherA2.[34] As shown previously,[35] HAR allows for the position of the bridging hydride to be defined, as well as discussion of its associated bond lengths and angles. Further details can be found in the SI.[36]

The dinuclear gallate anionic fragment in **4** is identical with that found in **2**, but because HAR could be applied to this structural determination, discussion of its most salient structural parameters is included here. It comprises two GaR_3 units connected by a bridging hydride, where each Ga center adopts a distorted tetrahedral geometry (the mean bond angles around Ga1 and Ga2 are 109.16° and 109.29°, respectively). The Ga1−H−Ga2 bond angle [134.6(9)°] is

https://doi.org/10.1021/acs.inorgchem.1c01276
Inorg. Chem. XXXX, XXX, XXX−XXX

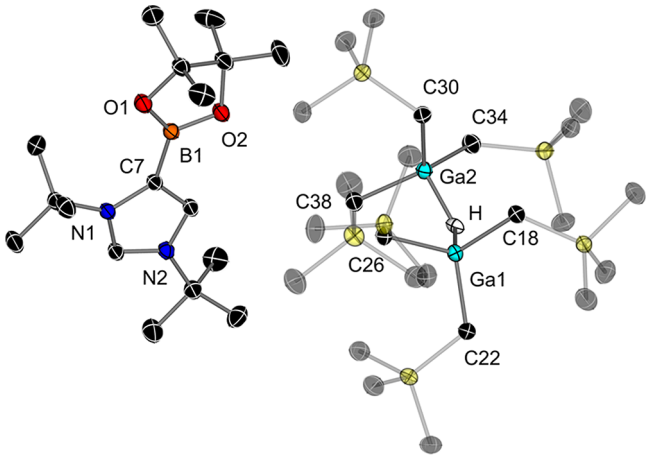

Figure 4. Molecular structure of **4** with displacement ellipsoids at 50% probability with H atoms omitted for clarity, with the exception of bridging hydride atoms. $SiMe_3$ groups have been drawn at 70% transparency for clarity. Selected bond angles (deg) and distances (Å) for **4**: Ga1−H−Ga2 134.6(9), O1−B1−C7 129.24(10), O1−B1−O2 114.39(10), C7−B1−O2 116.35(10), B1−C7−N1 133.86(9), B1−C7−C8 120.53(9), N1−C7−C8 105.61(9), H−Ga1−C26 107.3(5), H−Ga1−C22 102.0(5), H−Ga1−C18 102.0(5), C26−Ga1−C22 114.41(5), C26−Ga1−C18 115.74(5), Ga1−H−Ga2 134.6(9); B1−C7 1.5648(15), Ga1−C26 2.0201(11), Ga1−C22 2.0156(11), Ga1−C18 2.0177(11), Ga1−H 1.783(16), Ga2−H 1.770(17).

noticeably more acute than that reported by Stephan et al. for a phosphonium gallate, $[\{Ga(C_6F_5)_3(\mu\text{-}H)Ga(C_6F_5)_3\}^-]$ [175(2)°].[27] It should be noted that there are currently only a few known species of structurally defined anionic gallium(III) hydride.[27,37] Related to the anion present in **2** and **4**, Uhl et al. reported the structure of neutral Np_2GaH (Np = CH_2CMe_3), which in the solid state exhibits a dimeric motif.[38] The gallate anion of **4** is balanced by a cation that can be considered to be a structural isomer of that present in **2**, where the BPin fragment now resides on the C4 position. A slight shortening of the C−B bond is observed compared to that in **2** [C2−BPin 1.588(3) Å (**2**) vs C7−BPin 1.5648 (15) Å (**4**)], reflecting the stronger σ-donor abilities of the mesoionic carbene and its lower steric demands.[39] Additionally, the BPin ring now resides in the same plane as the imidazole ring, as opposed to its perpendicular disposition in **2**. The unexpected formation of **4** can perhaps be explained by the occurrence of thermally induced frustration, facilitating breakage of the Ga−C bond at elevated temperatures and enabling trapping of the C4 isomer by its reaction with HBPin.[31] C2- and C4-bound isomers have been previously detected by us for the activation of 4-bromobenzaldehyde, where it was found that insertion of the aldehyde between the Lewis acidic/basic fragments was thermodynamically favored toward the C4 position.[8]

Interestingly, **4** also seems to be highly reactive in solution, and attempts to characterize this species by NMR spectroscopy by dissolving isolated crystals of **4** in C_6D_6 led to the observation of 2 equiv of free GaR_3 alongside a new set of resonances at 6.85, 4.40, 1.35, and 0.86 ppm in a 1:2:9:9 ratio, which we attribute to $[H_2C\{[N(t\text{Bu})]_2CHCBPin\}]$ (**5**; Scheme 3b). The isolation of **5** can be understood as a decomposition pathway of gallate **4**, where now the dinuclear gallate anion of the ion pair can act as a nucleophile toward the C2 position of the cationic fragment $\{a\text{It}\text{Bu-BPin}\}^+$, formally reducing the cation and leading to neutral **5**.

Despite the observed decomposition pathways, the ability to form species **2** and **4** shows that these compounds are at least short-lived in solution. Given that gallium hydrides have shown some precedence within recent literature toward catalytic hydrogenation[27] and hydroboration reactions,[40] the presence of a Ga−H fragment within **2** lends potential for it to exhibit similar reductive behavior via hydroboration processes.

When benzophenone (**6**) was chosen as a model substrate, early stages within the optimization studies revealed that the combined action of I*t*Bu and GaR_3 was necessary to promote hydroboration, with quantitative conversion to **7a** observed after 20 min at room temperature (Table 1, entry 4). Lowering

Table 1. Catalyst Screening for Hydroboration of 6 by HBPin[a]

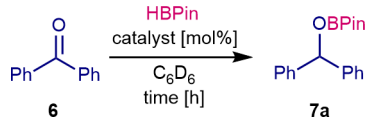

6 **7a**

entry	catalyst	loading(mol %)	time (h)	yield of **7a** (%)
1	none	-	12	50[b]
2	GaR_3	5	3.5	30
3	I*t*Bu	5	2	16
4	I*t*Bu + GaR_3	10	0.3	>99
5	**I*t*Bu + GaR_3**	**5**	**3.5**	**>99**
6	IPr·GaR_3	5	3.5	3
7	*a*I*t*Bu·GaR_3	10	14	37
8	*a*I*t*Bu·GaR_3	5	1.5	>99[b]
9	I*t*Bu + $GaCl_3$	5	3.5	12
10	**3**	5	3.5	43

[a]Reactions were performed in a J. Young NMR tube at 1 mmol scale in 0.5 mL of C_6D_6. All reactions were performed at room temperature unless otherwise stated, with yields determined against a 10 mol % C_6Me_6 internal standard by ^1H NMR spectroscopy. [b]Reactions were performed at 70 °C.

the catalyst loading to 5 mol % of each component (entry 5) allowed for >99% of **7a** to be formed after 3.5 h under ambient conditions. Demonstrating the catalytic superiority of the I*t*Bu and GaR_3 partnership, entry 6 shows that the NHC-GaR_3-stable C2 adduct, IPr·GaR_3 [IPr = 1,3-bis(2,6-diisopropylphenyl)imidazol-2-ylidene],[23] is unable to carry out the conversion, highlighting the need for the Lewis pair to be uncomplexed, and act cooperatively. The same outcome was observed with *a*I*t*Bu·GaR_3 (entry 7); however, increasing the reaction temperature to 70 °C allowed for quantitative conversion to **7a** (entry 8). Altering the tris(alkyl)gallium for a less bulky, yet stronger Lewis acid ($GaCl_3$, entry 9) did not improve the efficiency of the reaction, reaffirming the value in the steric incompatibility between the Lewis acid and Lewis base components. Finally, the neutral abnormal NHC **3** was employed as a catalyst because it is the direct decomposition product of ion pair **2**. Hydroboration was observed to be very sluggish, suggesting it is unlikely to play a key role in mediating these reactions, under the conditions of this study.

Under the optimized conditions of 5 mol % of both GaR_3 and I*t*Bu, the protocol could be expanded toward a selection of ketones and aldehydes (Figure 5). Acetophenone was quantitatively transformed into **7b** within 2.5 h at room temperature. However, when pronounced steric bulk was introduced to the ketone, i.e., with 2,2-dimethylpropiophenone, the reaction time was seen to significantly increase to 19

https://doi.org/10.1021/acs.inorgchem.1c01276
Inorg. Chem. XXXX, XXX, XXX−XXX

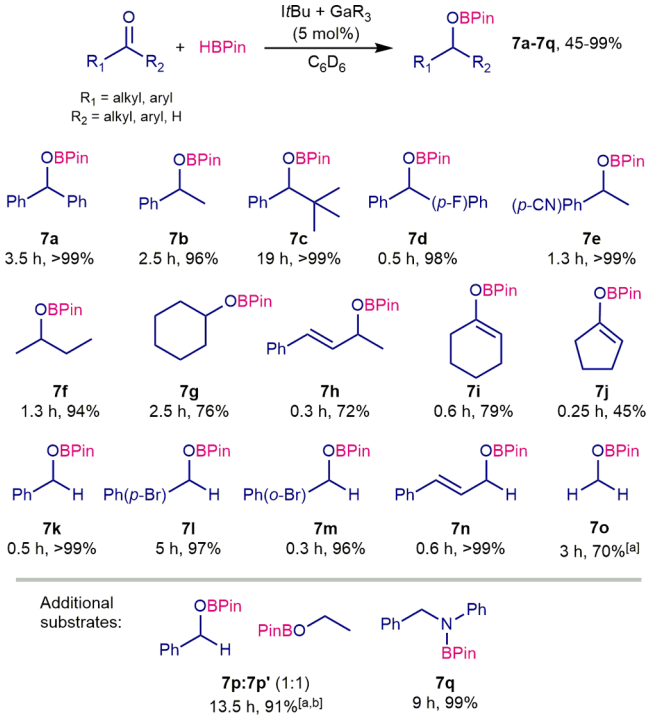

Figure 5. Scope of ItBu/GaR_3-catalyzed hydroboration. Reactions performed in a J. Young NMR tube at 1 mmol scale in 0.5 mL of C_6D_6. All reactions were performed at room temperature unless otherwise stated, with yields determined against a 10 mol % C_6Me_6 internal standard by ^{1}H NMR spectroscopy. [a]Reactions were performed at 70 °C. [b]2 equiv of HBPin was employed.

h (**7c**, >99%). The high yields obtained for **7d** in just 30 min demonstrate halide tolerance within the catalysis because no interfering side reactions were detected. Highlighting the chemoselectivity of this process, the introduction of a sensitive nitrile group (**7e**) sees the reaction occurring selectively at the carbonyl function; additionally, the reduced reaction time compared to **7a** could be a consequence of the electron-withdrawing properties of the CN functionality. Closing the ketone scope, aliphatic 2-butanone readily underwent hydroboration at room temperature in a short time (**7f**, 1.3 h, 94%), and cyclohexanone also displayed conversion into its analogous product (**7g**) in a respectable yield of 76%. A slight reduction in the chemoselectivity was observed with benzylideneacetone. Although the majority of hydroboration occurred in a 1,2 fashion across the carbonyl function (**7h**, 72%), a 10% yield of the product of the addition across the alkene (**7h′**) was also observed by NMR spectroscopy (see the SI). Upon moving to the cyclic α,β-unsaturated ketones (**7i** and **7j**), 1,4-hydroboration was exclusively achieved. We also exposed a selection of aldehydes to the catalytic conditions. Benzaldehyde, and its bromo-substituted derivatives, proved to undergo hydroboration very effectively and selectively at room temperature (**7k**–**7m**). The cinnamaldehyde reaction proceeded with excellent chemoselectivity (contrasting with its ketone derivative) reaching 99% conversion to **7n** in just 40 min. The product from the hydroboration of paraformaldehyde (**7o**) was obtained in 70% yield after 3 h at 70 °C.

We also assessed the ability of this NHC/GaR_3 system to catalyze the hydroboration of ethylbenzoate, which led to cleavage of the C–O bond to generate **7p** and **7p′** in a 1:1 ratio. The reaction was carried out by employing 2 equiv of HBPin and a slight elevation of temperature (70 °C; see the SI for details).[36] We were also successful in the quantitative hydroboration of *N*-benzylideneaniline, creating a N–B bond in the process (**7q**, 99%) visible by ^{11}B NMR spectroscopy with the appearance of a broad singlet at 25.3 ppm.

Although catalytic hydroboration through an FLP approach has been investigated in previous cases,[21,22] the unsaturated molecules involved prior to this work were imines and alkynes. The various aldehydes and ketones discussed here show the diversity that the ItBu/GaR_3 system can offer, while exhibiting high functional group tolerance and good chemoselectivity. Despite this varied carbonyl-based scope, the system was found to be inactive toward alkenes and alkynes.

Appreciating that **2** could potentially be involved during the catalytic cycle, the presence of a metal hydride fragment within

Scheme 4. Control Reactions: (a) Synthesis of 8 from the the Reaction between [ItBuOCH$_2$GaR$_3$] and HBPin; (b) Hydroboration of 6 Using 9 as a Catalyst; (c) Hydroboration of 6 Using 10 as a Catalyst

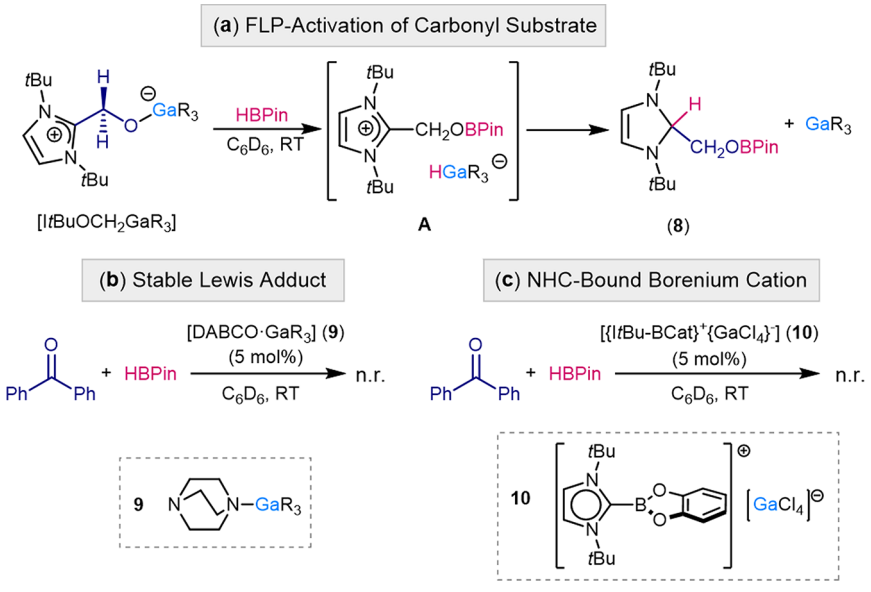

https://doi.org/10.1021/acs.inorgchem.1c01276
Inorg. Chem. XXXX, XXX, XXX–XXX

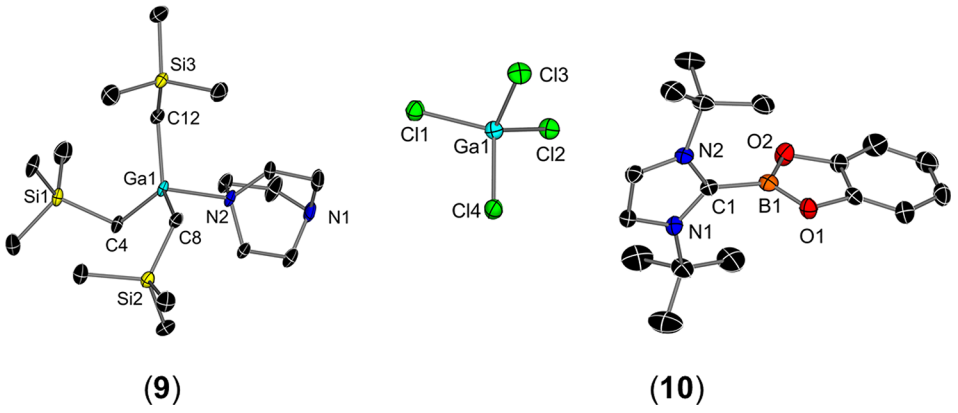

Figure 6. Molecular structures of **9** and **10** with displacement ellipsoids at 50% probability for **9** and 30% probability in **10**. All H atoms have been omitted for clarity. Selected bond angles (deg) and lengths (Å) of **9**: C12−Ga1−N2 100.12(9), C4−Ga1−N2 101.85(9), C8−Ga1−N2 101.80(9); N2−Ga1 2.150(2). Selected bond angles (deg) and lengths (Å) of **10**: N2−C1−B1 127.7(7), B1−C1−N2 125.7(7); C1−B1 1.569(11).

this species prompted us to consider that a classical σ-bond metathesis route could be in operation, led through an initial addition of the substrate across the [{Ga−H}$^-$] bond and then generation of the product triggered by the reaction of HBPin across the alkoxide intermediate. However, it must also be acknowledged that the countercation of **2**, [{I*t*Bu-BPin}$^+$], cannot be assumed to be completely innocent, given the literature precedence for Lewis base-stabilized borenium cations to catalyze hydroboration and hydrosilylation reactions.[21,41] We had to consider the following: (i) if BPin$^+$ could dissociate from [I*t*Bu-BPin}$^+$], a catalytically viable borenium cation would be liberated in solution, and (ii) [{I*t*Bu-BPin}$^+$] could be responsible for quenching a gallium alkoxide intermediate and lead to the formation of the boronate ester product rather than remaining as a spectator ion. Appreciating the complexity of the three-component system (GaR_3, I*t*Bu, and HBPin) under study, we elected to conduct a series of control reactions and kinetic investigations, in order to deduce a potential catalytic pathway and gain an increased understanding of the transformation at hand.

MECHANISTIC STUDIES

The optimization stage of this study confirmed that the presence of both I*t*Bu and GaR_3 was key to achieving efficient reactivity, lending a further suggestion that traditional FLP reactivity is likely occurring at some stage within the hydroboration process. Acknowledging that unsaturated substrates such as aldehydes and ketones can undergo insertion between I*t*Bu and GaR_3, we first considered the possibility that, rather than the initial FLP splitting of HBPin, a converse scenario involving activation of the carbonyl substrate could instead be occurring. In order to test this hypothesis, zwitterionic [I*t*BuCH_2OGaR_3] was prepared (by reacting equimolar amounts of paraformaldehyde, I*t*Bu, and GaR_3),[8] and reacted with 1 equiv of HBPin in C_6D_6 (Scheme 4a). Monitoring the reaction by ^{11}B NMR spectroscopy revealed conversion of the characteristic doublet attributable to HBPin (28.5 ppm) into a broad singlet at 22.5 ppm, consistent with the formation of a B−O bond. Analysis of the ^{1}H NMR spectrum revealed the quantitative formation of boronic ester (**8**) instead of the 1,2-addition product **7o**. The ^{1}H NMR spectra of this reaction mixture showed an informative triplet at 4.47 ppm for the CH fragment in **8** formed by reduction of the original C2 position of the imidazolium ring in [I*t*BuCH_2OGaR_3], whereas the protons of the unsaturated backbone resonate at 5.37 ppm (Figure S38). Along with **8**, the presence of free GaR_3 was also observed. Formation of **8** can be rationalized considering the initial σ-bond metathesis of the O−Ga bond in [I*t*BuCH_2OGaR_3] by HBPin to give a putative imidazolium gallate hydride **A** (Scheme 4a), which evolves in a manner similar to that described for **4**, via hydride addition to the C2 position of the imidazolium ring to form **8**. These findings suggest that preactivation of carbonyl-containing substrates by I*t*Bu/GaR_3 seems unlikely to be a true step involved in the catalytic hydroboration processes.

In order to glean more information into the role of the Lewis acid, the stoichiometric reactivity between GaR_3 and HBPin revealed that, after 15 days at room temperature in C_6D_6, GaR_2H is quantitatively formed alongside BPin-R (^{11}B NMR, 33.8 ppm). Despite the presence of a metal hydride here, subsequent reactivity with **6** was sluggish, mirroring the diminished catalytic activity found when using GaR_3 in the absence of its bulky partner, I*t*Bu (Table 1, entry 2), and supporting the key role of the formation of an anionically activated gallate hydride to favor the hydroboration process. The enhanced reactivity of the gallate hydride species versus neutral hydride complexes has also been noticed by Mulvey et al.[16c] as well as Thomas and Cowley for the hydroboration of alkynes using a variety of Al precatalysts such as $AlEt_3$ and $LiAlH_4$.[17b] This poor reactivity of GaR_3 on its own contrasts markedly with the proficiency of the Lewis acid B[3,5-$(CF_3)_2$-$C_6H_3]_3$ toward the hydroboration of alkenes, as reported by Oestreich et al.,[19,42] where redistribution between the tris(aryl)borane and HBPin promotes the formation of catalytically active, electron-deficient hydroboranes in solution. However, the authors comment that subtle changes to the characteristics of the Lewis acid can greatly affect the overall reactivity, where $B(C_6F_5)_3$ was found to be catalytically incompetent under the same conditions.

Attention was then turned to the cationic fragment of **2**, [{I*t*Bu-BPin}$^+$], which could not be assumed to be inert without further study. Crudden and co-workers established that FLP activation of HBPin led to the ion pair [{DABCO-BPin}$^+${H-B$(C_6F_5)_3$}$^-$], with mechanistic studies disclosing that the borenium cation of this species was the true mediator in the catalytic hydroboration of imines regardless of the nature of the counteranion and was reliant on the ability of the borenium ion to dissociate from the Lewis base.[21] Given the constitutional similarities between [{DABCO-BPin}$^+${H-B-

https://doi.org/10.1021/acs.inorgchem.1c01276
Inorg. Chem. XXXX, XXX, XXX−XXX

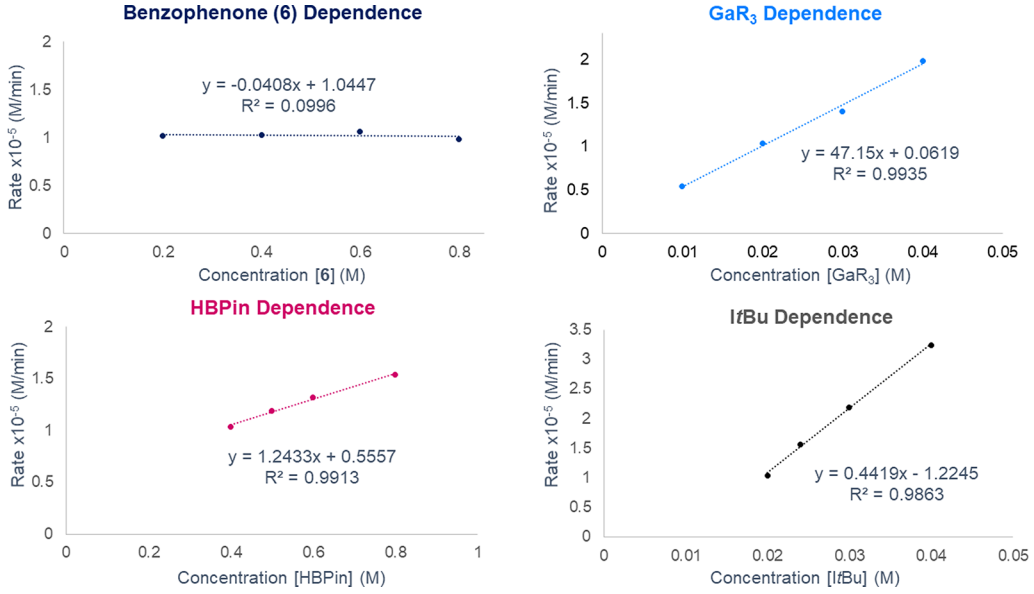

Figure 7. Kinetic profiles of the initial rate determination of catalysis components. Results show the first-order dependence in GaR_3, HBPin, and I*t*Bu, with a zeroth-order dependence detected in **6**.

$(C_6F_5)_3\}^-]$ and **2**, it was fitting that we considered a similar cationic dependence within our system. Taking an approach similar to that of Crudden et al. and upon substitution of the Lewis base I*t*Bu for DABCO in the reaction with GaR_3 and HBPin, it was found that the FLP reactivity was suppressed and instead formation of the Lewis adduct [DABCO·GaR_3] (**9**) was favored (Figure 6). Compound **9** exhibits structural parallels to [DABCO·$AlEt_3$], as reported by Cowley et al.,[17a] with the only distinct structural difference being in the bond length between the Lewis base and metal center, where the Al−N distance is notably shorter than the Ga−N bond of **9** [2.054(4) vs 2.150(2) Å], which highlights the large steric demand of the CH_2SiMe_3 groups. The authors then describe the ability of [DABCO·$AlEt_3$] to mediate hydroboration of alkynes and alkenes by the generation of a reactive aluminum hydride species. However, in our hands, **9** did not exhibit any reactivity with HBPin under stoichiometric conditions, and when its catalytic ability was probed by reacting HBPin and **6**, it was found that the relevant hydroboration product **7o** could not be detected at room temperature (Scheme 4b), with a modest yield of 23% only reachable when harsher reaction conditions were employed (70 °C, 16 h; Figure S28).[37]

Altering our approach, we elected to introduce Cl-BCat to equimolar amounts of I*t*Bu and $GaCl_3$ in hexane at room temperature, which allowed for cleavage of the B−Cl bond to result in $[\{ItBu\text{-}BCat\}^+\{GaCl_4\}^-]$ (**10**), which contains a cation similar to that found in **2** (Figure 6). Crystallographic features show that the $[\{GaCl_4\}^-]$ anion is in a near-ideal tetrahedral geometry with an average bond angle of 109.46° and Ga−Cl bond lengths ranging from 2.169(2) to 2.180(2) Å, which are typical for this specific anion.[43] Within the cationic component, $[\{ItBu\text{-}BCat\}^+]$, the C1−B1 bond length of 1.569(11) Å is similar to those detected previously for compounds **2** and **4** [C25−B1 1.588(5) Å (**2**) and C4−B1 1.563(4) Å (**4**)] and in good agreement with a related compound reported by Vidović et al. comprised of this same cation balanced by a $[\{B(3,5\text{-}Cl_2\text{-}C_6H_3)_4\}^-]$ anion and previously discussed herein.[25] The multinuclear NMR spectroscopic data for **10** are also consistent with those previously reported.[25] Additionally, the geometry at B was found to be in a distorted trigonal-planar environment, with the sum of its internal angles being 359° and no evidence of any interactions between the B center and the $[\{GaCl_4\}^-]$ anion.

With a suitable cation in hand, **10** was then used to shed light on the potential role of the cationic moiety within the catalysis. Spectroscopic investigations between **10** and a 20-fold excess of **6** showed the appearance of a new set of **6** resonances in the ^{1}H NMR spectrum and the appearance of a new NHC environment, hinting that a minor degree of displacement of NHC coordination in favor of the ketone may indeed be possible. This can be rationalized by the substantial Lewis acidity present at the B center, which is a known characteristic feature of borenium cations,[44] and the fact that borenium cations are known, under certain conditions, to dissociate from their partnered Lewis base.[45] The oxophilicity of borenium cations has also been demonstrated by Ingleson et al., given the propensity for $[\{Et_3N\text{-}BCat\}^+]$ to bind to the O atom of $Et_3P{=}O$ in the measurement of its Lewis acidity via the Gutmann−Beckett method.[46] Studies by Piers et al. also support these observations, where Lewis acidic boranes have been shown to bind to the O atom of carbonyl-based substrates, activating them toward subsequent reduction.[47] Introducing 1 equiv of HBPin to **6** and 5 mol % **10** displayed no onward reactivity, suggesting the need for a hydridic anion to also be present in order for hydroboration to occur (Scheme 4c).

The results, thus far, highlight not only that I*t*Bu and GaR_3 are both essential for reactivity but also that pathways based exclusively on the borenium cation can be ruled out. Further details were gathered by kinetic analyses under reaction conditions similar to those employed in the catalytic procedure (Figure 7). ^{1}H NMR monitoring of the reduction of **6** with HBPin mediated by 5 mol % of each I*t*Bu and GaR_3 revealed an overall first-order decay. In agreement with this, the initial rate methods showed a first-order dependence in each HBPin, GaR_3, and I*t*Bu, with a zeroth-order behavior detected in **6**. It is worth noting that an observed first-order dependence on

https://doi.org/10.1021/acs.inorgchem.1c01276
Inorg. Chem. XXXX, XXX, XXX−XXX

GaR_3 is in line with our initial hypothesis that the inclusion of a second entity of GaR_3 within the anionic fragment of **2** is most likely a feature of the solid-state constitution of this species. In fact, one could expect that a possible monoanionic $\{GaR_3H\}^-$ species, containing a terminal hydride, would be significantly more nucleophilic that the anion found in **2**.

On the basis of these observations, we can cautiously propose the catalytic cycle shown in Figure 8. Facilitated by

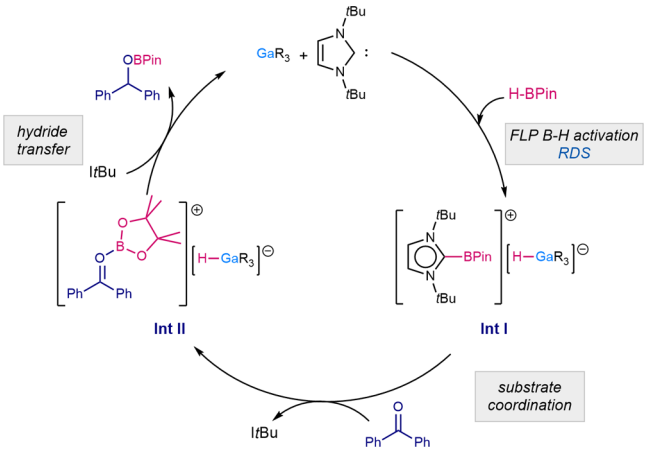

Figure 8. Proposed catalytic cycle for FLP-mediated hydroboration of unsaturated substrates. R = CH_2SiMe_3.

the FLP-activating properties of the I*t*Bu/GaR_3 combination toward HBPin, the first step is likely to involve cleavage of the B−H bond of the hydroborane and give rise to **Int I**, akin to **2**. This can be considered to be the rate-determining step of the reaction in view of the first-order dependence established for each of these species from the initial rate measurements. The absence of a detectable induction period with our kinetic analyses indicates that cleavage of HBPin is an on-cycle event. The inability to study the solution behavior of **2** lends weight to the fact that this borenium/hydride ion pair is highly reactive. While we cannot ascertain from our experiments the definite abilities of the cation, our results imply that partial dissociation of $BPin^+$ from I*t*Bu can occur in the presence of an excess of a carbonyl-containing substrate. This would allow for transformation between short-lived **Int I** and **Int II**, leading to borenium activation of the carbonyl and facilitating hydride transfer from $\{GaR_3\text{-}H\}^-$, release of the target product, and regeneration of the precatalysts I*t*Bu and GaR_3. Similar pathways involving preactivation of the substrates prior to reduction have shown precedence within catalytic hydrosilylation[41] reactions and in the FLP-catalyzed hydrogenation of imines.[48]

Appreciating that the formation of **Int II** would likely be driven by the oxophilicity of B, it is fitting to also acknowledge that $[\{I\textit{t}Bu\text{-}BPin\}^+]$ could assume the role of an in situ quenching agent toward a gallium alkoxide anion, succeeding insertion of the ketone across the Ga−H bond of **Int I** (Figure S55). Employing **10** as a cationic surrogate to **2** and reacting it with the anionic alkoxide LiOEt indicated a significant degree of oxophilicity of the cation due to the formation of EtO-BCat by multinuclear NMR spectroscopy in tetrahydrofuran (THF)-d_8.[37] However, it should be noted that the inability to isolate ion pair **2** and to test its reactivity toward **6** or its potential catalytic ability renders the mechanistic proposal shown in Figure 8 as tentative.

In an effort to explore other potential avenues that could be involved, we have also considered the possibility of BH_3 acting as a catalyst. Previous studies into the nucleophilic decomposition of hydroboranes revealed that the unexpected presence of BH_3 or hydridoboranes, BH_4^- and $B_2H_7^-$, can often be "Trojan horses" within catalytic hydroboration reactions and be more realistic mediators of the transformation.[15,49] However, it was found that the hydroboration of **6** with HBPin in the presence of 5 mol % BH_3·THF did not proceed under our optimized conditions or even after heating at 70 °C for 1 h (Table S1 and Figure S30).[36] Within the system at hand, it is therefore unlikely that BH_3 or any related hydridoboranes are performing competing catalytic pathways.

CONCLUSIONS

In conclusion, we have progressed the FLP capabilities of I*t*Bu/GaR_3 (R = CH_2SiMe_3) by activation of the commodity hydroborating reagent, HBPin, and reported the first catalytic applications of this LB/LA combination for the efficient hydroboration of aldehydes and ketones. The initial stoichiometric studies led to the isolation and structural authentication of reactive ion pair **2** resulting from FLP splitting of the B−H bond of the borane. An unprecedented reactivity of the abnormal carbene complex **1** with HBPin at elevated temperatures was also unveiled, resulting in the isolation of a structural isomer of **2**, i.e., **4**. Compounds **2** and **4** showed to be highly reactive in solution—evolving at room temperature into the abnormal NHC-Ga complex **3** and dihydroimidazole **5**, respectively. Thorough mechanistic studies (including kinetic investigations) suggest that the ion pair **Int I** is the active species of this process. Coordination and activation of the substrate to the borenium cation of this pair have been proposed to occur, increasing the electrophilicity of the C═O bond and prompting subsequent reduction by the $[\{GaR_3\text{-}H\}^-]$ fragment to yield the final product. Despite the existing precedence for catalytic applications of FLP splitting of hydroboranes, this study reinforces that the catalytic pathways involved appear to be unique to the Lewis acid/base pairing used and system-specific. This is dually highlighted by several control reactions and kinetic investigations, the results of which suggest a cooperative mechanism that we have tentatively proposed. Emphasis must also be placed on the mechanistic difference between conventional main-group hydride catalysts (which typically proceed through a σ-bond metathesis pathway) and the borenium gallate hydride established herein; appreciating the potential of the $[I\textit{t}Bu\text{-}BPin]^+$ fragment rather than only acknowledging the Ga−H bond allowed for the design of informative control experiments. While borenium cations themselves are known to be excellent promotors within various catalytic transformations, this study also demonstrates the importance of the hydridic nature of the anion and its instrumental role in catalytic turnover.

EXPERIMENTAL SECTION

All procedures were conducted using standard Schlenk-line and glovebox techniques under an inert atmosphere of argon. Solvents [pentane, hexane, toluene, and diethyl ether (Et_2O)] were degassed, purified, and collected via an MBraun SPS 5 and stored over 4 Å molecular sieves for at least 24 h prior to use. THF was dried by heating to reflux over a sodium wire/benzophenone ketyl radical and stored over 4 Å molecular sieves for 24 h prior to use. Deuterated solvents (C_6D_6, THF-d_8, and toluene-d_8) were purchased from VWR,

https://doi.org/10.1021/acs.inorgchem.1c01276
Inorg. Chem. XXXX, XXX, XXX−XXX

dried over a NaK alloy for 16 h, and then cycled through three rounds of degassing by employing a freeze−pump−thaw method. The deuterated solvents were then collected via vacuum transfer and stored under an argon atmosphere over 4 Å molecular sieves. HBPin was purchased from Fluorochem, stored in an argon-sealed ampule, and cycled through three rounds of degassing by employing a freeze−pump−thaw method. Substrates **4a−4q** were purchased from Sigma-Aldrich, Fluorochem, or Alfa-Aesar; liquids were stored over 4 Å molecular sieves for 24 h prior to use. DABCO and phenol were purchased from Sigma-Aldrich, sublimed before use, and stored in a glovebox under an argon atmosphere. NMR spectra were recorded on Bruker spectrometers operating at either 300 or 400 MHz. ^{1}H NMR spectra: 300.1 or 400.1 MHz. ^{13}C{^{1}H} NMR spectra: 75.5 or 100.6 MHz. ^{19}F NMR spectra: 282.4 MHz. $Ga(CH_2SiMe_3)_3$,[50] I*t*Bu,[51] *a*I*t*Bu·GaR_3 (**1**)[23] were prepared according to literature methods.

Synthesis of [{I*t*Bu-BPin}$^+${GaR_3(μ-H)GaR_3}$^-$] (2; R = CH_2SiMe_3). To an argon-prepared Schlenk flask was added 1 mmol (0.33 g) of GaR_3 dissolved in 5 mL of pentane, and the resulting solution was cooled to 0 °C, followed by the addition of 1 mmol (0.15 mL) of HBPin. Then, an equimolar amount of I*t*Bu (1 mmol, 0.180 g) was added, and a fine white suspension was obtained. This mixture was stirred at 0 °C for 1 h, resulting in a colorless solution, which was then concentrated in vacuo, to approximately 1 mL of solvent. Cooling to −30 °C afforded a crop of colorless crystals, determined as **2** by X-ray diffraction. Repeated attempts at the isolation of **2** for analyses beyond X-ray diffraction led to the inevitable formation of an abnormal NHC-Ga complex, [BPinC{[N(*t*Bu)]$_2$CHCGa(R)$_3$}] (**3**), which cocrystallizes alongside GaR_3 and *a*I*t*Bu·GaR_3. Yield: 110 mg, 17% (MW = 637.63). Anal. Calcd for $C_{29}H_{64}BGaN_2O_2Si_3$: C, 54.45; H, 10.40; N, 4.38. Found: C, 53.59; H, 10.64; N, 4.70. ^{1}H NMR (298 K, C_6D_6): δ 7.32 (s, 1H, imidazole backbone), 1.64 (s, 9H, *t*Bu), 1.26 (s, 9H, *t*Bu), 1.01 (s, 12H, CH_3, BPin), 0.33 (s, 27H, CH_3, R), −0.22 (s, 6 H, CH_2, R). ^{11}B NMR (298 K, C_6D_6): δ 28.63 (C2-BPin). ^{13}C NMR (298 K, C_6D_6): δ 160.3 (NC(BPin)N), 129.1 (*C*H, imidazole backbone), 86.2 (C_q, BPin), 61.2 (*C*(CH$_3$)$_3$), 58.7 (*C*(CH$_3$)$_3$), 31.9 (*C*H$_3$, *t*Bu), 30.7 (*C*H$_3$, *t*Bu), 25.6 (*C*H$_3$, BPin), 3.8 (*C*H$_3$, R), 2.6 (*C*H$_2$, R).

Synthesis of [{*a*I*t*Bu-BPin}$^+${GaR_3(μ-H)GaR_3}$^-$] (4; R = CH_2SiMe_3). A total of 1 mmol (0.513 g) of *a*I*t*Bu·GaR_3 was dissolved in 5 mL of hexane, followed by the addition of 1 mmol (0.15 mL) of HBPin. This mixture was heated to reflux for 4 h, resulting in a colorless solution. This solution was then concentrated in vacuo, to approximately 1 mL of solvent. Cooling to −30 °C afforded a crop of colorless crystals, determined as **4** by X-ray diffraction. Repeated attempts at the isolation of **4** for analyses beyond X-ray diffraction led to reduction of the cationic fragment to give [H$_2$C{[N(*t*Bu)]$_2$CHCBPin}] (**5**). Yield: 83 mg, 27% (MW = 308.27). Anal. Calcd for $C_{17}H_{33}BN_2O_2$: C, 66.24; H, 10.79; N, 9.09. Found: C, 64.48; H, 10.69; N, 8.66. ^{1}H NMR (298 K, C_6D_6): δ 6.92 (s, 1H, imidazole backbone), 4.43 (s, 2H, C2-*H*$_2$), 1.35 (s, 9H, *t*Bu), 1.12 (s, 12H, C*H*$_3$, BPin), 0.86 (s, 9H, *t*Bu). ^{11}B NMR (298 K, C_6D_6): δ 29.0 (C4-*B*). ^{13}C NMR (298 K, C_6D_6): δ 140.6 (NC(BPin)N), 129.1 (CH, imidazole backbone), 82.4 (C_q, BPin), 68.2 (C2-H$_2$), 55.6 (*C*(CH$_3$)$_3$), 51.8 (*C*(CH$_3$)$_3$), 31.9 (residual hex.), 27.9 (*C*H$_3$, *t*Bu), 27.5 (*C*H$_3$, *t*Bu), 24.8 (*C*H$_3$, BPin), 23.0 (residual hex.), 14.3 (residual hex.).

Synthesis of [DABCO·GaR_3] (9; R = CH_2SiMe_3). In a Schlenk flask, 1 mmol (0.33 g) of GaR_3 was dissolved in 10 mL of hexane under an argon atmosphere, followed by the addition of 1 mmol (0.15 mL) of HBPin. To this was added an equimolar amount of DABCO (1 mmol, 0.112 g), resulting in a colorless solution. The mixture was allowed to stir at room temperature for 3 h and then concentrated under reduced pressure to give a white suspension. Applying gentle heating regained a colorless solution, which, upon slow cooling to room temperature, resulted in a crop of colorless crystals. Measurement by X-ray diffraction revealed the product to be Lewis adduct **9**. Yield: 0.222 g, 50% (MW = 443.55). Anal. Calcd for $C_{18}H_{45}GaN_2Si_3$: C, 48.74; H, 10.23; N, 6.32. Found: C, 48.14; H, 10.27; N, 6.47. ^{1}H NMR (298 K, C_6D_6): δ 2.24 (s, 12H, CH_2, DABCO), 0.30 (s, 27H, CH_3, R), −0.61 (s, 6H, CH_2, R). ^{13}C{^{1}H} NMR (298 K, C_6D_6): δ 45.9 (CH$_2$, DABCO), 3.2 (CH$_3$, R), 0.3 (CH$_2$, R).

Synthesis of [{I*t*Bu-BCat}$^+${$GaCl_4$}$^-$] (10). In an argon-prepared Schlenk flask, 1 mmol (0.176 g) of $GaCl_3$ was dissolved in 10 mL of hexane, followed by the addition of 1 mmol (0.154 g) of Cl-BCat,[52] giving a colorless solution. The addition of an equimolar amount of I*t*Bu (0.180 g) gave a white suspension, which was allowed to stir at room temperature for 5 h. The removal of all volatiles under reduced pressure gave a white solid, which was then redissolved in 5 mL of toluene with gentle heating; a colorless solution and a small amount of orange oil were then obtained. Slow cooling to room temperature produced a crop of colorless crystals, which were determined to be **10**. Yield: 0.314 g, 61% (MW = 510.72). Anal. Calcd for $Cl_4GaC_{17}H_{24}BN_2O_2$: C, 39.98; H, 4.74; N, 5.49. Found: C, 38.72. H; 4.77; N, 5.68. ^{1}H NMR (298 K, C_6D_6/THF-d_8): δ 7.54 (s, 2H, C*H*, imidazole backbone), 7.28 (m, 2H, C_{Ar}-*H*), 7.07 (m, 2H, C_{Ar}-*H*), 1.27 (s, 18H, CH_2, *t*Bu). ^{11}B NMR (298 K, C_6D_6/THF-d_8): δ 27.8 (br s, {I*t*Bu-*B*Cat}$^+$). ^{13}C{^{1}H} NMR (298 K, C_6D_6/THF-d_8): δ 146.8 (C-*B*Cat), 125.6 (C_{Ar}−H), 123.4 (*C*-H, imidazole backbone), 120.8 (C_q), 114.3 (C_{Ar}−H), 62.6 (*C*(CH$_3$)$_3$), 30.2 (C(*C*H$_3$)$_3$).

GENERAL CATALYTIC PROCEDURE

Reactions were performed in a J. Young NMR tube at 2.0 M C_6D_6 with 1 mmol of substrate and 1.05 mmol (0.15 mL) of HBPin. A total of 0.05 mmol (9 mg, 5 mol %) of I*t*Bu and 0.05 mmol (17 mg, 5 mol %) of GaR_3 (or the relevant catalyst according to Table 1) were added and the reactions monitored by multinuclear NMR spectroscopy until evolution ceased.

ASSOCIATED CONTENT

Supporting Information

The Supporting Information is available free of charge at https://pubs.acs.org/doi/10.1021/acs.inorgchem.1c01276.

General methods, synthetic procedures, X-ray crystallographic details, synthesis of compounds **2**, **4**, **9**, and **10**, catalyst optimization, procedures for catalytic hydroboration, stoichiometric reactions and mechanistic investigations, kinetic measurements, an alternative catalytic pathway, and spectra of compounds **7a−7q** (PDF)

Accession Codes

CCDC 2080195−2080200 contain the supplementary crystallographic data for this paper. These data can be obtained free of charge via www.ccdc.cam.ac.uk/data_request/cif, or by emailing data_request@ccdc.cam.ac.uk, or by contacting The Cambridge Crystallographic Data Centre, 12 Union Road, Cambridge CB2 1EZ, UK; fax: +44 1223 336033.

AUTHOR INFORMATION

Corresponding Author

Eva Hevia − *Department für Chemie, Biochemie und Pharmazie, Universität Bern, Bern CH3012, Switzerland;* orcid.org/0000-0002-3998-7506; Email: eva.hevia@dcb.unibe.ch

Authors

Leonie J. Bole − *Department für Chemie, Biochemie und Pharmazie, Universität Bern, Bern CH3012, Switzerland*

Marina Uzelac − *Department of Pure and Applied Chemistry, University of Strathclyde, Glasgow G1 1XL, United Kingdom*

Alberto Hernán-Gómez − *Departamento de Química Orgánica y Química Inorgánica, Universidad de Alcalá, Alcalá de Henares-Madrid 28805, Spain*

https://doi.org/10.1021/acs.inorgchem.1c01276
Inorg. Chem. XXXX, XXX, XXX−XXX

Alan R. Kennedy − *Department of Pure and Applied Chemistry, University of Strathclyde, Glasgow G1 1XL, United Kingdom;* orcid.org/0000-0003-3652-6015
Charles T. O'Hara − *Department of Pure and Applied Chemistry, University of Strathclyde, Glasgow G1 1XL, United Kingdom;* orcid.org/0000-0002-1691-1568

Complete contact information is available at: https://pubs.acs.org/10.1021/acs.inorgchem.1c01276

Author Contributions

The manuscript was written through contributions of all authors. All authors have given approval to the final version of the manuscript.

Notes

The authors declare no competing financial interest.

■ ACKNOWLEDGMENTS

We thank the University of Bern and the SNF (Grant 188573) for the generous sponsorship of this research. The X-ray crystal structure determination service unit of the Department of Chemistry and Biochemistry of the University of Bern is acknowledged for measuring, solving, refining, and summarizing the structures of compounds **3** and **4**. The Synergy diffractometer was partially funded by the SNF within the R'Equip programme (Project 206021_177033). A.H.-G. acknowledges the Comunidad de Madrid and Universidad de Alcalá for the funding through the Research Talent Attraction Program (2018-T1/AMB-11478) and Programa Estímulo a la Investigación de Jovenes Investigadores (CM/JIN/2019-030).

■ REFERENCES

(1) (a) Brown, H. C.; Schlesinger, H. I.; Cardon, S. Z.m Studies in Stereochemistry. I. Steric Strains as a Factor in the Relative Stability of Some Coordination Compounds of Boron. *J. Am. Chem. Soc.* **1942**, *64*, 325. (b) Welch, G. C.; Juan, R. R. S.; Masuda, J. D.; Stephan, D. W. Reversible, Metal-Free Hydrogen Activation. *Science* **2006**, *314*, 1124.

(2) (a) Stephan, D. W. Frustrated Lewis Pairs: From Concept to Catalysis. *Acc. Chem. Res.* **2015**, *48*, 306. (b) Stephan, D. W. Frustrated Lewis Pairs. *J. Am. Chem. Soc.* **2015**, *137*, 10018.

(3) (a) Stephan, D. W.; Erker, G. Frustrated Lewis Pairs: Metal-Free Hydrogen Activation and More. *Angew. Chem., Int. Ed.* **2010**, *49*, 46. (b) Hounjet, L. J.; Stephan, D. W. Hydrogenation by Frustrated Lewis Pairs: Main Group Alternatives to Transition Metal Catalysts? *Org. Process Res. Dev.* **2014**, *18*, 385.

(4) (a) Dureen, M. A.; Lough, A.; Gilbert, T. M.; Stephan, D. W. B−H Activation by Frustrated Lewis Pairs: Borenium or Boryl Phosphonium Cation? *Chem. Commun.* **2008**, *36*, 4303. (b) Chase, P. A.; Stephan, D. W. Hydrogen and Amine Activation by a Frustrated Lewis Pair of a Bulky N-Heterocyclic Carbene and $B(C_6F_5)_3$. *Angew. Chem., Int. Ed.* **2008**, *47*, 7433. (c) Erős, G.; Mehdi, H.; Pápai, I.; Rokob, T. A.; Király, P.; Tárkányi, G.; Soós, T. Expanding the Scope of Metal-Free Catalytic Hydrogenation through Frustrated Lewis Pair Design. *Angew. Chem., Int. Ed.* **2010**, *49*, 6559. (d) Ghattas, G.; Bizzarri, C.; Hölscher, M.; Langanke, J.; Gürtler, C.; Leitner, W.; Subhani, M. A. Interaction of Formaldehyde with a Water-Tolerant Frustrated Lewis Pair. *Chem. Commun.* **2017**, *53*, 3205.

(5) (a) Holschumacher, D.; Bannenberg, T.; Hrib, C. G.; Jones, P. G.; Tamm, M. Heterolytic Dihydrogen Activation by a Frustrated Carbene-Borane Lewis Pair. *Angew. Chem., Int. Ed.* **2008**, *47*, 7428. (b) Kolychev, E. L.; Bannenberg, T.; Freytag, M.; Daniliuc, C. G.; Jones, P. G.; Tamm, M. Reactivity of a Frustrated Lewis Pair and Small-Molecule Activation by an Isolable Arduengo Carbene-B{3,5-$(CF_3)_2C_6H_3$}$_3$ Complex. *Chem. - Eur. J.* **2012**, *18*, 16938. (c) Ashley, A. E.; Thompson, A. L.; O'Hare, D. Non-Metal-Mediated Homogeneous Hydrogenation of CO_2 to CH_3OH. *Angew. Chem., Int. Ed.* **2009**, *48*, 9839.

(6) (a) Ménard, G.; Tran, L.; McCahill, J. S. J.; Lough, A. J.; Stephan, D. W. Contrasting the Reactivity of Ethylene and Propylene with P/Al and P/B Frustrated Lewis Pairs. *Organometallics* **2013**, *32*, 6759. (b) Appelt, C.; Slootweg, J. C.; Lammertsma, K.; Uhl, W. Reaction of a P/Al-Based Frustrated Lewis Pair with Ammonia, Borane, and Amine-Boranes: Adduct Formation and Catalytic Dehydrogenation. *Angew. Chem., Int. Ed.* **2013**, *52*, 4256. (c) Uhl, W.; Appelt, C. Reactions of an Al−P-Based Frustrated Lewis Pair with Carbonyl Compounds: Dynamic Coordination of Benzaldehyde, Activation of Benzoyl Chloride, and Al−C Bond Cleavage with Benzamide. *Organometallics* **2013**, *32*, 5008.

(7) Abdalla, J. A. B.; Riddlestone, I. M.; Tirfoin, R.; Aldridge, S. Cooperative Bond Activation and Catalytic Reduction of Carbon Dioxide at a Group 13 Metal Center. *Angew. Chem., Int. Ed.* **2015**, *54*, 5098.

(8) Uzelac, M.; Armstrong, D. R.; Kennedy, A. R.; Hevia, E. Understanding the Subtleties of Frustrated Lewis Pair Activation of Carbonyl Compounds by N-Heterocyclic Carbene/Alkyl Gallium Pairings. *Chem. - Eur. J.* **2016**, *22*, 15826.

(9) Uzelac, M.; Kennedy, A. R.; Hevia, E. Trans-Metal-Trapping Meets Frustrated-Lewis-Pair Chemistry: $Ga(CH_2SiMe_3)_3$-Induced C−H Functionalizations. *Inorg. Chem.* **2017**, *56*, 8615.

(10) Schnee, G.; Nieto Faza, O.; Specklin, D.; Jacques, B.; Karmazin, L.; Welter, R.; Silva López, C.; Dagorne, S. Normal-to-Abnormal NHC Rearrangement of Al^{III}, Ga^{III}, and In^{III} Trialkyl Complexes: Scope, Mechanism, Reactivity Studies, and H_2 Activation. *Chem. - Eur. J.* **2015**, *21*, 17959.

(11) Chong, C. C.; Kinjo, R. Catalytic Hydroboration of Carbonyl Derivatives, Imines, and Carbon Dioxide. *ACS Catal.* **2015**, *5*, 3238.

(12) Shegavi, M. L.; Bose, S. K. Recent Advances in the Catalytic Hydroboration of Carbonyl Compounds. *Catal. Sci. Technol.* **2019**, *9*, 3307.

(13) (a) Arrowsmith, M.; Hill, M. S.; Hadlington, T.; Kociok-Köhn, G.; Weetman, C. Magnesium-Catalyzed Hydroboration of Pyridines. *Organometallics* **2011**, *30*, 5556. (b) Arrowsmith, M.; Hadlington, T. J.; Hill, M. S.; Kociok-Köhn, G. Magnesium-Catalysed Hydroboration of Aldehydes and Ketones. *Chem. Commun.* **2012**, *48*, 4567. (c) Arrowsmith, M.; Hill, M. S.; Kociok-Köhn, G. Magnesium Catalysis of Imine Hydroboration. *Chem. - Eur. J.* **2013**, *19*, 2776. (d) Weetman, C.; Hill, M. S.; Mahon, M. F. Magnesium-Catalysed Hydroboration of Isonitriles. *Chem. Commun.* **2015**, *51*, 14477. (e) Weetman, C.; Hill, M. S.; Mahon, M. F. Magnesium Catalysis for the Hydroboration of Carbodiimides. *Chem. - Eur. J.* **2016**, *22*, 7158. (f) Weetman, C.; Anker, M. D.; Arrowsmith, M.; Hill, M. S.; Kociok-Köhn, G.; Liptrot, D. J.; Mahon, M. F. Magnesium-Catalysed Nitrile Hydroboration. *Chem. Sci.* **2016**, *7*, 628.

(14) Yang, Z.; Zhong, M.; Ma, X.; De, S.; Anusha, C.; Parameswaran, P.; Roesky, H. W. An Aluminum Hydride That Functions like a Transition-Metal Catalyst. *Angew. Chem., Int. Ed.* **2015**, *54*, 10225.

(15) Harder, S.; Spielmann, J. Calcium-Mediated Hydroboration of Alkenes: "Trojan Horse" or "True" Catalysis? *J. Organomet. Chem.* **2012**, *698*, 7.

(16) Pollard, V. A.; Orr, S. A.; McLellan, R.; Kennedy, A. R.; Hevia, E.; Mulvey, R. E. Lithium Diamidodihydridoaluminates: Bimetallic Cooperativity in Catalytic Hydroboration and Metallation Applications. *Chem. Commun.* **2018**, *54*, 1233. (b) Pollard, V. A.; Fuentes, M. Á.; Kennedy, A. R.; McLellan, R.; Mulvey, R. E. Comparing Neutral (Monometallic) and Anionic (Bimetallic) Aluminum Complexes in Hydroboration Catalysis: Influences of Lithium Cooperation and Ligand Set. *Angew. Chem., Int. Ed.* **2018**, *57*, 10651. (c) Pollard, V. A.; Young, A.; McLellan, R.; Kennedy, A. R.; Tuttle, T.; Mulvey, R. E. Lithium-Aluminate-Catalyzed Hydrophosphination Applications. *Angew. Chem., Int. Ed.* **2019**, *58*, 12291.

(17) (a) Bismuto, A.; Thomas, S. P.; Cowley, M. J. Aluminum Hydride Catalyzed Hydroboration of Alkynes. *Angew. Chem., Int. Ed.* **2016**, *55*, 15356. (b) Bismuto, A.; Cowley, M. J.; Thomas, S. P.

Aluminum-Catalyzed Hydroboration of Alkenes. *ACS Catal.* **2018**, *8*, 2001.
(18) Fleige, M.; Mobus, J.; vom Stein, T.; Glorius, F.; Stephan, D. W. Lewis Acid Catalysis: Catalytic Hydroboration of Alkynes Initiated by Piers' Borane. *Chem. Commun.* **2016**, *52*, 10830.
(19) Yin, Q.; Kemper, S.; Klare, H. F. T.; Oestreich, M. Boron Lewis Acid-Catalyzed Hydroboration of Alkenes with Pinacolborane: $BArF_3$ Does What $B(C_6F_5)_3$ Cannot Do! *Chem. - Eur. J.* **2016**, *22*, 13840.
(20) (a) Yin, Q.; Soltani, Y.; Melen, R. L.; Oestreich, M. $BArF_3$-Catalyzed Imine Hydroboration with Pinacolborane Not Requiring the Assistance of an Additional Lewis Base. *Organometallics* **2017**, *36*, 2381. (b) Lawson, J. R.; Wilkins, L. C.; Melen, R. L. Tris(2,4,6-Trifluorophenyl)Borane: An Efficient Hydroboration Catalyst. *Chem. - Eur. J.* **2017**, *23*, 10997. (c) Carden, J. L.; Gierlichs, L. J.; Wass, D. F.; Browne, D. L.; Melen, R. L. Unlocking the Catalytic Potential of Tris(3,4,5-Trifluorophenyl)Borane with Microwave Irradiation. *Chem. Commun.* **2019**, *55*, 318.
(21) Eisenberger, P.; Bailey, A. M.; Crudden, C. M. Taking the F out of FLP: Simple Lewis Acid-Base Pairs for Mild Reductions with Neutral Boranes via Borenium Ion Catalysis. *J. Am. Chem. Soc.* **2012**, *134*, 17384.
(22) Vasko, P.; Zulkifly, I. A.; Fuentes, M. Á.; Mo, Z.; Hicks, J.; Kamer, P. C. J.; Aldridge, S. Reversible C−H Activation, Facile C−B/B−H Metathesis and Apparent Hydroboration Catalysis by a Dimethylxanthene-Based Frustrated Lewis Pair. *Chem. - Eur. J.* **2018**, *24*, 10531.
(23) Uzelac, M.; Hernán-Gómez, A.; Armstrong, D. R.; Kennedy, A. R.; Hevia, E. Rational Synthesis of Normal, Abnormal and Anionic NHC-Gallium Alkyl Complexes: Structural, Stability and Isomerization Insights. *Chem. Sci.* **2015**, *6*, 5719.
(24) (a) Silva Valverde, M. F.; Schweyen, P.; Gisinger, D.; Bannenberg, T.; Freytag, M.; Kleeberg, C.; Tamm, M. N-Heterocyclic Carbene Stabilized Boryl Radicals. *Angew. Chem., Int. Ed.* **2017**, *56*, 1135. (b) Matsumoto, T.; Gabbai, F. P. A Borenium Cation Stabilized by an N-Heterocyclic Carbene Ligand. *Organometallics* **2009**, *28*, 4252.
(25) Bhunia, M.; Sahoo, S. R.; Das, A.; Ahmed, J.; Sreejyothi, P.; Mandal, S. K. Transition Metal-Free Catalytic Reduction of Primary Amides Using an Abnormal NHC Based Potassium Complex: Integrating Nucleophilicity with Lewis Acidic Activation. *Chem. Sci.* **2020**, *11*, 1848.
(26) Do, D. C. H.; Muthaiah, S.; Ganguly, R.; Vidović, D. Synthesis of N-Heterocyclic Carbene Stabilized Catecholatoborenium Cations by Ligand Substitution. *Organometallics* **2014**, *33*, 4165.
(27) Xu, M.; Possart, J.; Waked, A. E.; Roy, J.; Uhl, W.; Stephan, D. W. Halogenated Triphenylgallium and -Indium in Frustrated Lewis Pair Activations and Hydrogenation Catalysis. *Philos. Trans. R. Soc., A* **2017**, *375*, 20170014.
(28) Aldridge, S.; Downs, A. J. *The Group 13 Metals Aluminium, Gallium, Indium and Thallium: Chemical Patterns and Peculiarities*; John Wiley & Sons, Ltd., 2011.
(29) (a) Uzelac, M.; Kennedy, A. R.; Hevia, E.; Mulvey, R. E. Transforming LiTMP Lithiation of Challenging Diazines through Gallium Alkyl Trans-Metal-Trapping. *Angew. Chem.* **2016**, *128*, 13341. (b) McLellan, R.; Uzelac, M.; Kennedy, A. R.; Hevia, E.; Mulvey, R. E. LiTMP Trans-Metal-Trapping of Fluorinated Aromatic Molecules: A Comparative Study of Aluminum and Gallium Carbanion Traps. *Angew. Chem., Int. Ed.* **2017**, *56*, 9566.
(30) Holschumacher, D.; Bannenberg, T.; Hrib, C. G.; Jones, P. G.; Tamm, M. Heterolytic Dihydrogen Activation by a Frustrated Carbene-Borane Lewis Pair. *Angew. Chem., Int. Ed.* **2008**, *47*, 7428.
(31) Rokob, T. A.; Hamza, A.; Stirling, A.; Pápai, I. On the Mechanism of $B(C_6F_5)_3$-Catalyzed Direct Hydrogenation of Imines: Inherent and Thermally Induced Frustration. *J. Am. Chem. Soc.* **2009**, *131*, 2029.
(32) Jayatilaka, D.; Dittrich, B. X-Ray Structure Refinement Using Aspherical Atomic Density Functions Obtained from Quantum-Mechanical Calculations. *Acta Crystallogr., Sect. A: Found. Crystallogr.* **2008**, *64*, 383.
(33) Capelli, S. C.; Bürgi, H. B.; Dittrich, B.; Grabowsky, S.; Jayatilaka, D. Hirshfeld Atom Refinement. *IUCrJ* **2014**, *1*, 361.
(34) Kleemiss, F.; Dolomanov, O. V.; Bodensteiner, M.; Peyerimhoff, N.; Midgley, L.; Bourhis, L. J.; Genoni, A.; Malaspina, L. A.; Jayatilaka, D.; Spencer, J. L.; White, F.; Grundkötter-Stock, B.; Steinhauer, S.; Lentz, D.; Puschmann, H.; Grabowsky, S. Accurate Crystal Structures and Chemical Properties from NoSpherA2. *Chem. Sci.* **2021**, *12*, 1675.
(35) Woińska, M.; Grabowsky, S.; Dominiak, P. M.; Woźniak, K.; Jayatilaka, D. Hydrogen Atoms Can Be Located Accurately and Precisely by X-Ray Crystallography. *Sci. Adv.* **2016**, *2*, e1600192.
(36) See the SI for further details.
(37) (a) Hallock, R. B.; Beachley, O. T.; Li, Y. J.; Sanders, W. M.; Churchill, M. R.; Hunter, W. E.; Atwood, J. L. A Reexamination of the Reactions of $Ga(CH_2SiMe_3)_3$ and $In(CH_2SiMe_3)_3$ with Alkali-Metal Hydrides. The Search for a Reductive-Elimination Reaction. *Inorg. Chem.* **1983**, *22*, 3683. (b) Veith, M.; Burkhart, M.; Huch, V. Magnesium Bis(Tetrahydridogallate(III)): Structure and Reaction with Tert-Butyl. *Angew. Chem., Int. Ed.* **2006**, *45*, 5544. (c) Linti, G.; Çoban, S.; Rodig, A.; Sandholzer, N. Siliciumhaltige Ringverbindungen Des Galliums Und Indiums — Neue Hydridogallanate. *Z. Anorg. Allg. Chem.* **2003**, *629*, 1329.
(38) Uhl, W.; Cuypers, L.; Geiseler, G.; Harms, K.; Massa, W. Synthesen Und Kristallstrukturen von Dialkylgalliumhydriden - Dimere versus Trimere Formeleinheiten. *Z. Anorg. Allg. Chem.* **2002**, *628*, 1001.
(39) Vivancos, Á.; Segarra, C.; Albrecht, M. Mesoionic and Related Less Heteroatom-Stabilized N-Heterocyclic Carbene Complexes: Synthesis, Catalysis, and Other Applications. *Chem. Rev.* **2018**, *118*, 9493.
(40) (a) Ford, A.; Woodward, S. Catalytic Enantioselective Reduction of Ketones by a Chiral Gallium Complex and Catecholborane. *Angew. Chem., Int. Ed.* **1999**, *38*, 335. (b) Blake, A. J.; Cunningham, A.; Ford, A.; Teat, S. J.; Woodward, S. Enantioselective Reduction of Prochiral Ketones by Catecholborane Catalysed by Chiral Group 13 Complexes. *Chem. - Eur. J.* **2000**, *6*, 3586.
(41) Rawat, S.; Bhandari, M.; Porwal, V. K.; Singh, S. Hydrosilylation of Carbonyls Catalyzed by Hydridoborenium Borate Salts: Lewis Acid Activation and Anion Mediated Pathways. *Inorg. Chem.* **2020**, *59*, 7195.
(42) Carden, J. L.; Dasgupta, A.; Melen, R. L. Halogenated Triarylboranes: Synthesis, Properties and Applications in Catalysis. *Chem. Soc. Rev.* **2020**, *49*, 1706.
(43) (a) Townsend, N. S.; Shadbolt, S. R.; Green, M.; Russell, C. A. Phosphacycles as Building Blocks for Main Group Cages. *Angew. Chem.* **2013**, *125*, 3565. (b) Weigand, J. J.; Riegel, S. D.; Burford, N.; Decken, A. Prototypical Phosphorus Analogues of Ethane: General and Versatile Synthetic Approaches to Hexaalkylated P-P Diphosphonium Cations. *J. Am. Chem. Soc.* **2007**, *129*, 7969.
(44) Piers, W. E.; Bourke, S. C.; Conroy, K. D. Borinium, Borenium, and Boronium Ions: Synthesis, Reactivity, and Applications. *Angew. Chem., Int. Ed.* **2005**, *44*, 5016.
(45) Schneider, W. F.; Narula, C. K.; Nöth, H.; Bursten, B. E. Structure and Bonding Trends in Two- and Three-Coordinate Boron Cations. *Inorg. Chem.* **1991**, *30*, 3919.
(46) Clark, E. R.; Del Grosso, A.; Ingleson, M. J. The Hydride-Ion Affinity of Borenium Cations and Their Propensity to Activate H2 in Frustrated Lewis Pairs. *Chem. - Eur. J.* **2013**, *19*, 2462.
(47) (a) Parks, D. J.; Blackwell, J. M.; Piers, W. E. Studies on the Mechanism of $B(C_6F_5)_3$ -Catalyzed Hydrosilation of Carbonyl Functions. *J. Org. Chem.* **2000**, *65*, 3090. (b) Parks, D. J.; Piers, W. E.; Parvez, M.; Atencio, R.; Zaworotko, M. J. Synthesis and Solution and Solid-State Structures of Tris(Pentafluorophenyl)Borane Adducts of PhC(O)X (X = H, Me, OEt, NPr^i_2). *Organometallics* **1998**, *17*, 1369.
(48) Chase, P. A.; Jurca, T.; Stephan, D. W. Lewis Acid-Catalyzed Hydrogenation: $B(C_6F_5)_3$-Mediated Reduction of Imines and Nitriles with H_2. *Chem. Commun.* **2008**, *2*, 1701.

https://doi.org/10.1021/acs.inorgchem.1c01276
Inorg. Chem. XXXX, XXX, XXX−XXX

(49) Ang, N.; Buettner, C.; Docherty, S.; Bismuto, A.; Carney, J.; Docherty, J.; Cowley, M.; Thomas, S. Borane-Catalysed Hydroboration of Alkynes and Alkenes. *Synthesis* **2018**, *50*, 803.
(50) Beachley, O. T.; Simmons, R. G. Preparation and Properties of ((Trimethylsilyl)Methyl)Gallium(III) Compound. *Inorg. Chem.* **1980**, *19*, 1021.
(51) Arduengo, A. J.; Krafczyk, R.; Schmutzler, R.; Craig, H. a.; Goerlich, J. R.; Marshall, W. J.; Unverzagt, M. Imidazolylidenes, Imidazolinylidenes and Imidazolidines. *Tetrahedron* **1999**, *55*, 14523.
(52) Reid, W. B.; Spillane, J. J.; Krause, S. B.; Watson, D. A. Direct Synthesis of Alkenyl Boronic Esters from Unfunctionalized Alkenes: A Boryl-Heck Reaction. *J. Am. Chem. Soc.* **2016**, *138*, 5539.

https://doi.org/10.1021/acs.inorgchem.1c01276
Inorg. Chem. XXXX, XXX, XXX−XXX